# Detection of Quantum Noise from an Electrically Driven Two-Level System

**Richard Deblock,*† Eugen Onac, Leonid Gurevich, Leo P. Kouwenhoven†**

The electrical noise of mesoscopic devices can be strongly influenced by the quantum motion of electrons. To probe this effect, we have measured the current fluctuations at high frequency (5 to 90 gigahertz) using a superconductor-insulator-superconductor tunnel junction as an on-chip spectrum analyzer. By coupling this frequency-resolved noise detector to a quantum device, we can measure the high-frequency, nonsymmetrized noise as demonstrated for a Josephson junction. The same scheme is used to detect the current fluctuations arising from coherent charge oscillations in a two-level system, a superconducting charge qubit. A narrow band peak is observed in the spectral noise density at the frequency of the coherent charge oscillations.

Electrical noise, or fluctuations in the current, has proved to be a powerful tool to probe mesoscopic devices (*1*). At high frequency, it can bear strong signatures of the dynamics resulting from quantum mechanics. One of the simplest systems to study this effect is a two-level system (TLS) with two coupled quantum states, $|0\rangle$ and $|1\rangle$, that can form a coherent superposition, $\alpha|0\rangle + \beta|1\rangle$, with $\alpha$ and $\beta$ complex numbers (Fig. 1A). If this TLS is forced into state $|0\rangle$ at time equal to zero, the probability, $P_{|1\rangle} = |\beta|^2$, to find the system in state $|1\rangle$ oscillates in time with a frequency determined by the coupling strength. This prediction (*2*) has recently attracted much interest in the context of quantum computation, where TLSs form the physical realizations of the qubit building blocks. To determine the state of the qubit, some detection mechanism is needed. In the case of solid-state devices, the qubit state is often measured by means of the value of an electrical current (*3*). We are interested in the fluctuations in the read-out current and how these are affected by the oscillating time evolution of a qubit.

The central idea is illustrated in Fig. 1, B and C. Suppose an electron hops on a TLS and initially occupies state $|0\rangle$. Due to the coupling between the two states (dashed arrow), $P_{|1\rangle}$ starts to oscillate. The electron can leave the TLS toward the right only when $P_{|1\rangle}$ is high. A new electron then repeats the cycle. Thus, the outgoing current consists of charge injections that preferentially occur near odd integers times half the oscillation period after the previous tunneling event (Fig. 1C). The fluctuations in the current still bear this nonstochastic noise, and, instead of the usual white noise spectrum, a narrow band peak is expected at the frequency determined by the coupling strength.

The idea above is very general and theoretical predictions on narrow band noise exist for Bloch oscillations in a double quantum well (*4*), charge oscillations in superconducting (*5*) and semiconducting qubits (*6*), and electron spin resonance oscillations (*7*). The experimental detection is difficult as the frequency, $f$, of the coherent oscillations is typically in the GHz range in order to fulfill the condition $hf \gg k_B T$, where $k_B T$ is the thermal energy (*8*). We report a detection scheme from which we obtain the frequency-resolved spectral density of current noise in the range of 5 to 90 GHz (*9*).

Our detection scheme follows the ideas of (*10*, *11*): a quantum device is coupled on-chip to a detector that converts the high-frequency noise signal into a direct current (DC). The on-chip coupling provides a large frequency bandwidth (~100 GHz), whereas the conversion to DC allows standard amplification of the signal (*12*). Our detector is a superconductor-insulator-superconductor (SIS) tunnel junction (fig. S2), known to be a sensitive microwave detector and well established in astronomy measurements (*13*). For low-voltage bias, the gap ($\Delta$) in the density of states prohibits tunneling of quasi-particles. However, for a bias $V_{SIS}$, the absorption of a photon of energy $\hbar\omega$ that exceeds ($2\Delta$-$eV_{SIS}$), can assist tunneling (inset of Fig. 2B). This photon-assisted tunneling (PAT) current carries information on the number and the frequency of photons reaching the detector (*14*).

To validate our noise detection, we have first measured on a Josephson junction (Jj) for which the high-frequency fluctuations are well known (Fig. 2A) (*15*). A Josephson junction, biased such that $|eV_{Jj}| < 2\Delta$, generates an alternating current (AC) of frequency $f_{Jj} = 2eV_{Jj}/h$ (*16*, *17*). The AC fluctuations are capacitively coupled to the detector side, where voltage fluctuations build up across the SIS junction. These electromagnetic fluctuations form microwave photons, which can be absorbed by tunneling quasi-particles. The measured PAT current through the SIS detector is shown in Fig. 2B (black solid curve). A clear step in the current is seen at $V_{SIS} = 285$ μV. The derivative of this curve is a measure of the noise spectral density. Thus the noise of a Josephson junction is indeed found to be narrow band and, in this case, centered around $(2\Delta - eV_{SIS}) = 32.5$ GHz consistent with the expected frequency $f_{Jj} = 33.8$ GHz for $V_{Jj} = 70$ μV.

For a quantitative description, we consider an SIS junction subject to current fluctuations. The PAT current for a bias $eV_{SIS} < 2\Delta$ is given by (*18*)

$$I_{PAT}(V_{SIS}) = \int_0^{+\infty} d\omega \left(\frac{e}{\hbar\omega}\right)^2 |Z(\omega)|^2 S_I(-\omega) I_{SIS}(V_{SIS} + \hbar\omega/e) \qquad (1)$$

where $I_{SIS}(V_{SIS})$ is the SIS current without noise, $Z(\omega)$ is the transimpedance $[Z(\omega) = \{S_{V,SIS}(\omega)/S_I(\omega)\}^{1/2}$, i.e., voltage fluctuations

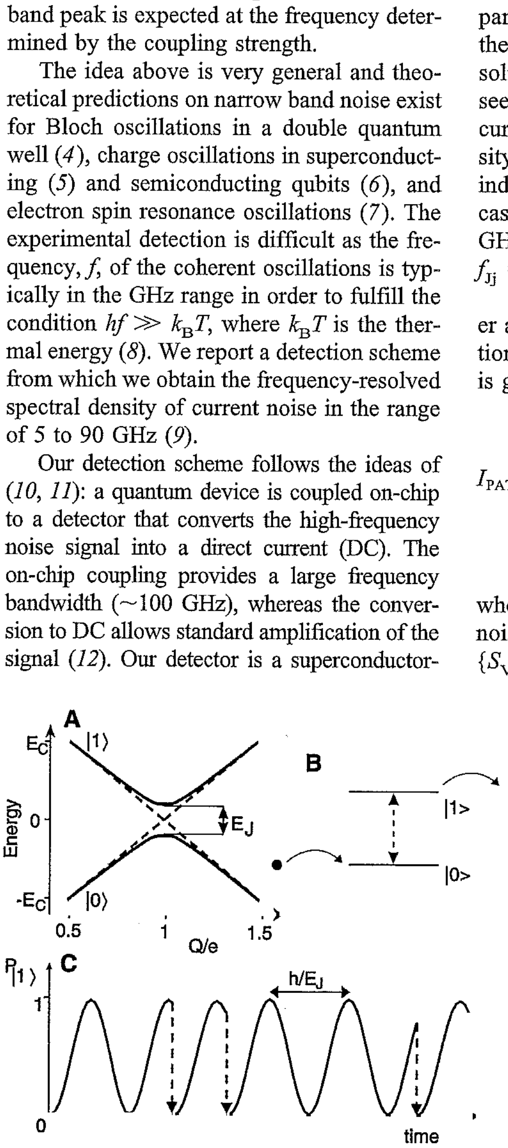


**Fig. 1.** (**A**) Energy diagram for a TLS with parameters for a superconducting charge qubit of charging energy $E_C$. $Q$ is the qubit charge. The charge states $|0\rangle$ and $|1\rangle$ are coupled by the Josephson energy, $E_J$, causing the bending of the dashed lines into the red solid curves. (**B**) A particular case of current flow via a TLS. (**C**) Schematic evolution of the probability to be in state $|1\rangle$ as a function of time. The collapses to the $|0\rangle$ state occur when the TLS is emptied. For a superconducting charge, qubit the oscillations have frequency $E_J/h$ and the collapse occurs by quasi-particle tunneling.

Department of Nanoscience and ERATO Mesoscopic Correlation Project, Delft University of Technology, Post Office Box 5046, 2600 GA Delft, Netherlands.

*Present address: Laboratoire de Physique des Solides, associé au CNRS, Université Paris-Sud, Bâtiment 510, 91 405 Orsay Cedex, France.

†To whom correspondence should be addressed. E-mail: deblock@ps.u-psud.fr (R.D.); leo@qt.tn.tudelft.nl (L.P.K.)

at the detector divided by current fluctuations from the source]. We emphasize that here the spectral density $S_I(\omega)$ corresponds to a non-symmetrized noise correlator (*10, 11, 19, 20*). Our SIS detector measures absorption of photons, which were emitted from the Josephson junction. Because the SIS detector itself is virtually noiseless for $eV_{SIS} < 2\Delta$, no emission from the detector occurs, and thus no absorption takes place in the Josephson junction. Under these conditions, we only measure the spectral density at (as commonly defined) negative frequencies, $S_I(-\omega)$ (*21*).

Equation 1 has been used to calculate the dashed curve in Fig. 2B, assuming a time-dependent current $I(t)=I_C \sin(2\pi f_{Jj}t)$ (or equivalently two delta-function noise peaks at $+f_{Jj}$ and $-f_{Jj}$). Using this AC Josephson current and the equation in (*18*), we recovered the standard equations for the PAT current [e.g. equation 3.4 of (*14*)]. The value of $Z(\omega)$ at $\omega = 2\pi f_{Jj}$ has been used as a fitting parameter in order to obtain good agreement with the experimental black solid curve of Fig. 2B. We have repeated this procedure for many different frequencies and, thus, obtained $Z(\omega)$ from 10 to 80 GHz (Fig. 3B). In this calculation, only the noise peak at $-f_{Jj}$ leads to a significant contribution to the PAT current (for $eV_{SIS} < 2\Delta$).

Biasing the Josephson junction, such that $eV_{Jj} > 2\Delta$, turns on quasi-particle tunneling. This tunneling is stochastic and gives rise to approximately white shot noise (*1, 22*). The SIS detector current (red solid curve of Fig. 2B) now appears very different from the narrow-band noise in the black solid curve. The dashed-dotted curve is calculated without any fit parameter. We have simply inserted $Z(\omega)$ (i.e., the red line in Fig. 3B) and the shot noise value, $S_I(\omega)= eI_{Jj}$ (*22*), in Eq. 1 and obtained good agreement with the experiment. Importantly, $S_I(\omega) = eI_{Jj}$ corresponds to the nonsymmetrized noise value (the symmetrized noise is the Poissonian value equal to $2eI_{Jj}$). The fact that only $eI_{Jj}$ fits our data demonstrates the first observation of nonsymmetrized noise in electrical conductors.

Figure 3A is a plot of the detector current versus $V_{Jj}$. The narrow-band AC Josephson noise and the white quasi-particle noise are clearly distinguishable with a transition at $|eV_{Jj}| = 2\Delta$. Figure 3C shows that the quasi-particle noise depends linearly on $I_{Jj}$, confirming the white shot noise character of this regime. We find that the resolution of this noise measurement is 80 fA$^2$/Hz, corresponding to an equivalent noise temperature of 3 mK on a 1 k$\Omega$ resistor.

To demonstrate narrow-band noise from an electrically driven qubit, we have chosen the Cooper Pair Box (CPB) as a physical realization of the TLS. The CPB is fabricated with the same aluminum technology as the SIS detector and, therefore, is easy to integrate on-chip (*15*). The two-levels, $|0>$ and $|1>$, correspond to $N$ and $N+1$ Cooper pairs in the box, which is controlled by the gate voltage $V_g$ (Fig. 4B, inset). The two levels are coupled by the Josephson energy, $E_J$, as illustrated in Fig. 1A (*3, 23*). The coherent charge oscillation corresponds to one extra Cooper pair tunneling on and off the box. When $P_{|1>}$ is high, a sudden decay to the $|0>$ state can take place by quasi-particle tunneling out of the qubit. The resulting current is expected to have narrow-band noise around a frequency $f = \sqrt{(4E_C(Q/e-1))^2+E_J^2}/h$ (*5*), which describes the energy difference between the two-levels in Fig. 1A. $E_C = e^2/2C_\Sigma$ is the charging energy, where $C_\Sigma$ is the total capacitance of the island and $Q = C_gV_g$ is the charge induced on the box. Because the decay is a stochastic process occurring around odd multiples times half the oscillation period, the narrow-band noise is not a delta peak as in the case of the AC Josephson effect. Instead, a broad peak is expected on top of a white shot noise background (*5*). The sudden quasi-particle decay is realized for bias and gate voltages near the so-called Josephson-QuasiParticle (JQP) peak (*3*). The average number of coherent charge oscillations is determined by the ratio $E_J/\Gamma$, where $\Gamma$ is the decay rate for the two quasi-particles (*24*). In our device, the Josephson

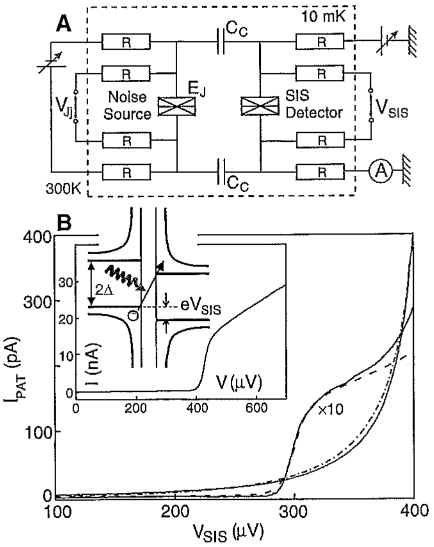


**Fig. 2.** (**A**) Circuit with SIS detector capacitively coupled to a Josephson junction acting as a noise source (*15*). Both sides are connected to room temperature equipment via on-chip resistances, $R \approx 2$ k$\Omega$ made from platinium wires (20 μm by 0.1 μm by 0.02 μm). The on-chip capacitances, $C_c \approx 550$ fF, have dimensions: area is 80 μm by 10 μm, and the silicon oxide insulator thickness is 50 nm. The circuit is mounted in a dilution refrigerator with base temperature 10 mK. (**B**) The black solid curve shows measured PAT current through the SIS detector for $V_{Jj} = 70$ μV. [$I_{PAT} \equiv I_{SIS}(V_{Jj}) - I_{SIS}(V_{Jj} = 0)$.] For the red solid curve, the Josephson junction is DC biased ($I_{Jj} = 100$ nA), such that quasi-particle tunneling generates the noise. Eq. 1 is used to fit the dashed line to the black curve, obtaining $Z(\omega)$, and to calculate without fit parameters the dashed-dotted curve. (Inset) Schematic energy diagram of PAT across an SIS junction. The curve is the bare $I_{SIS}$-$V_{SIS}$ characteristic (without noise), and the Josephson branch is suppressed by a magnetic flux due to the SQUID geometry of the detector, $2\Delta = 420$ μeV. From the sample parameters, we calculated the transimpedance $Z(\omega) \approx 900$ $\Omega$. This is an overestimation because it neglects the stray capacitances, for instance, from the Pt wires to ground.

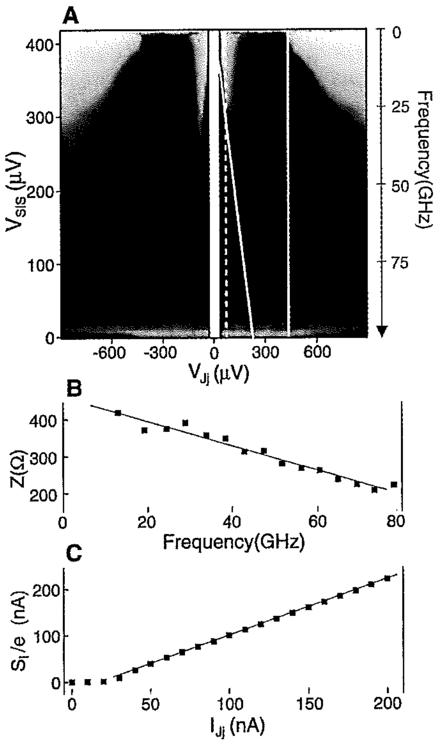


**Fig. 3.** (**A**) PAT current (logarithmic scale) versus $V_{Jj}$ and $V_{SIS}$. The right axis translates $V_{SIS}$ into frequency according to $f = (2\Delta - eV_{SIS})/h$. Zero current is black, and high current is pink. The current scale can be inferred from the black curve in Fig. 2B, which was taken at the white dashed line. The yellow line separates the region $|V_{Jj}| < 2\Delta/e = 420$ μV, dominated by emission from the AC Josephson effect at frequency $2eV_{Jj}/h$ (indicated by the white diagonal line), and the region $|V_{Jj}| > 420$ μV where shot noise is generated. The white area near $V_{Jj} = 0$ is not accessible, due to the Josephson branch of the Josephson junction. The feature near $V_{SIS} = 0$ μV is due to the remaining Josephson branch of the SIS detector. (**B**) Transimpedance, $Z(\omega)$, versus frequency deduced from fitting the PAT current generated by the AC Josephson effect. (**C**) Shot noise $S_I$ versus $I_{Jj}$. $S_I(I_{Jj})$ is deduced by scaling the dashed-dotted curve of Fig. 2B to fit the PAT current for different $I_{Jj}$. (For $I_{Jj} < 25$ nA the Josephson junction has not reached its normal state impedance, which causes the change in slope near the origin.)

junction has a superconducting quantum interference device (SQUID) geometry allowing to tune $E_J$. Consequently, we can explore both the coherent ($E_J > \Gamma$) and incoherent ($E_J < \Gamma$) regime.

The CPB (Fig. 4, B and C) is coupled to an SIS detector with the same on-chip circuitry as in Fig. 2 (fig. S1). First the CPB is characterized independently, and the JQP peak is identified (Fig. 4A, inset). Figure 4A shows measurements of the PAT current through the SIS detector for different CPB gate voltages. The PAT current is rather high on the left side ($Q/e < 1$) of the JQP peak and small on the right side ($Q/e > 1$). This is attributed to the emission character of the left side of the JQP peak versus absorption on the right (*25*). On the absorption side ($Q/e > 1$), the small PAT signal is attributed to tunneling processes not related to the coherent dynamics of the CPB, leading to a background PAT current. Indeed, because no energy is available flowing toward the CPB, the spectral density of the current fluctuations on the absorption side is virtually zero.

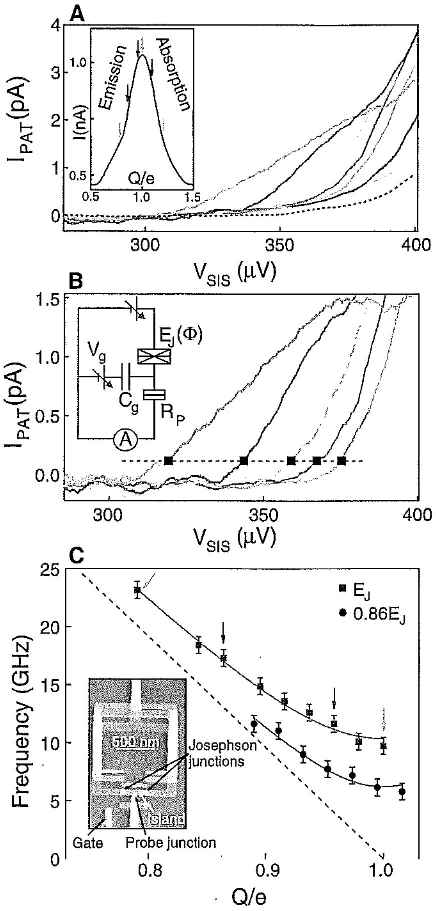


**Fig. 4.** (**A**) PAT current for different positions on the JQP peak, as indicated by arrows in the inset. Colored curves correspond to same-colored arrows. The dashed line corresponds to PAT current for $E_J/\Gamma < 1$. (Inset) Current versus charge, $Q$, for the CBP on the JQP peak. (**B**) PAT current after subtracting the PAT curve for $Q/e$=1.3. The squares correspond to the $V_{SIS}$ value used for the dominant frequency determination. (Inset) Schematic picture of CPB. The superconducting island is connected to a superconducting lead via a Josephson junction with $E_J$ tuneable by a magnetic flux $\Phi$. A resistive junction ($R_P$ = 335 kΩ) with negligible Josephson coupling is connected to the lower lead. A gate capacitance $C_g$ is used to modify the charge, $Q = C_g V_g$, on the island. (**C**) Dominant frequency deduced from the PAT current for two values of $E_J$. The solid lines are fits to the expression $\sqrt{(4E_C(Q/e-1))^2+E_J^2}/h$. The fit parameter $E_c$ = 100 μV is slightly higher than the measured charging energy. The arrows correspond to the points denoted on the inset of (A). (Inset) Photo of CPB device with $E_c$= 95 μV deduced from Coulomb blockade experiments.

On the left side, we observe more high-frequency components when moving away from the JQP peak center. To extract the noise component related to the JQP process, we subtract the small PAT current at high $Q$ (Fig. 4B). We then determined the dominant frequency component from the $V_{SIS}$ value where PAT became visible. (We checked the validity of this determination of the dominant frequency for the AC Josephson effect.) The $V_{SIS}$ values converted to frequencies were plotted versus $Q$ (Fig. 4C). The dominant frequency dependence on the charge on the CPB can be fitted by the energy difference between the two-levels of the CPB (solid curves in Fig. 4C). We obtained a charging energy slightly higher than expected. The dominant frequency value for $Q/e = 1$ is consistent with the value of $E_J$ in this sample [$E_J$ = 50 μeV = 12 GHz for maximum coupling (*26*)]. Changing $E_J$ (by means of the flux through the SQUID) changes the dominant frequency for $Q/e = 1$, as shown for the red data points. For small values of $E_J$, the PAT signal becomes very weak and has a shot noise shape similar to the PAT curves for $Q/e > 1$ (Fig. 4A). Indeed, in this incoherent regime ($\Gamma > E_J$), a dominant frequency from narrow-band noise is not expected.

We have demonstrated narrow-band, high-frequency detection of nonsymmetrized noise. The quantum noise from a charge qubit shows a peak at the frequency of the coherent charge oscillation. The SIS detector is operated as an on-chip spectrum analyzer and is applicable for correlation measurements on a wide range of electronic quantum devices.

### References and Notes


1. Y. M. Blanter, M. Büttiker, *Phys. Rep.* **336**, 1 (2000).
2. R. P. Feynman, *Lectures on Physics, vol. 3* (Addison-Wesley, Reading, MA, 1965).
3. Y. Nakamura, Yu. A. Pashkin, J. S. Tsai, *Nature* **398**, 786 (1999).
4. A. N. Korotkov, D. V. Averin, K. K. Likharev, *Phys. Rev. B* **49**, 7548 (1994).
5. M. S. Choi, F. Plastina, R. Fazio, *Phys. Rev. B* **67**, 045105 (2003).
6. R. Ruskov, A. N. Korotkov, *Phys. Rev. B* **67**, 075303 (2003), and references therein.
7. I. Martin, D. Mozyrsky, H. W. Jiang, *Phys. Rev. Lett.* **90**, 018301 (2003).
8. The condition $hf > k_BT$ is not required if the TLS is decoupled from phonons such as in spin systems. See, e.g., C. Durkan, M. E. Welland, *Appl. Phys. Lett.* **80**, 458 (2002).
9. There have been few measurements of the high-frequency symmetrized current noise (*27*, *28*).
10. R. Aguado, L. P. Kouwenhoven, *Phys. Rev. Lett.* **84**, 1986 (2000).
11. R. J. Schoelkopf *et al.*, e-Print available at http://xxx.lanl.gov/abs/cond-mat/0210247, and references therein.
12. Usually the bandwidth is in the kHz to MHz range, due to the long cabling between the low temperature device and room temperature equipment and additional filtering against room temperature noise.
13. SIS detectors are sensitive up to frequencies ~$2\Delta/h$. For aluminum junctions, which are used in this work, this is around 100 GHz. Niobium junctions are used in astronomy and go up to THz.
14. J. R. Tucker, M. J. Feldman, *Rev. Mod. Phys.* **57**, 1055 (1985).
15. The description of the sample is detailed in the supporting online material (SOM) Text.
16. M. Tinkham, *Introduction to Superconductivity* (McGraw-Hill, Singapore, ed. 2, 1996).
17. The oscillation amplitude is the critical current, $I_c = \pi\Delta/(2eR_N)$, where $R_N$ is the normal state resistance (*16*). In our sample $R_N$ = 14.1 kΩ; thus, $I_c$ = 23 nA.
18. Equation 1 follows from inserting eq. 5 in (*10*) into eq. 157 in (*29*). We obtain

$$I_{PAT}(V) = \int_0^{+\infty} d\omega \left(\frac{e}{\hbar\omega}\right)^2 |Z(\omega)|^2 S_I(-\omega) I\left(V_{SIS}+\frac{\hbar\omega}{e}\right) + \int_0^{eV} d\omega \left(\frac{e}{\hbar\omega}\right)^2 |Z(\omega)|^2 S_I(\omega) I\left(V_{SIS}-\frac{\hbar\omega}{e}\right) - \int_{-\infty}^{+\infty} d\omega \left(\frac{e}{\hbar\omega}\right)^2 |Z(\omega)|^2 S_I(\omega) I(V_{SIS})$$

The first term corresponds to emission from the device ($\omega < 0$), the second corresponds to absorption ($\omega > 0$), and the third renormalizes the elastic current. For $eV_{SIS} < 2\Delta$, only the first term is nonzero.
19. G. B. Lesovik, R. Loosen, *JETP Lett.* **65**, 295 (1997).
20. U. Gavish, Y. Levinson, Y. Imry, *Phys. Rev. B* **62**, R10637 (2000).
21. When $eV_{SIS} > 2\Delta$, the SIS detector is sensitive to $\omega > 0$. In this case, the PAT is a small correction on a large background current and difficult to measure.
22. Strictly speaking, the nonsymmetrized noise of a normal tunnel junction is not frequency-independent. For $eV > hf \gg kT$, one has $S_I(f) = eI(1+hf/eV)$ (*10*), where the frequency $f$ can be negative or positive. The quasi-particle branch occurs for $eV > 2\Delta$, which means that $eV > hf$ and, consequently, that the frequency- dependent part of $S_I(f)$ is negligible in our range of parameters. This has been checked numerically.
23. V. Bouchiat, D. Vion, P. Joyez, D. Estève, M. H. Devoret, *Physica Scripta T* **76**, 165 (1998).
24. From $\Gamma = (eV+E_C)/e^2R_P$, where $R_P$ is the probe junction resistance, we deduce $\Gamma$ = 2 GHz.
25. The strong asymmetry in the JQP peak regarding emission and absorption was observed by Y. Nakamura *et al.* (*30*). It is also consistent with recent theoretical predictions (*31*, *32*).
26. The evaluation of $R_J$ is difficult because $R_J$ is in series with $R_P$. It is estimated from similarly fabricated junctions with a 20% uncertainty.
27. R. H. Koch, D. J. Van Harlingen, J. Clarke, *Phys. Rev. Lett.* **47**, 1216 (1981).

28. R. J. Schoelkopf *et al.*, *Phys. Rev. Lett.* **78**, 3370 (1997).
29. G. L. Ingold, Yu. V. Nazarov, in *Single-Charge Tunneling*, H. Grabert, M. H. Devoret, Eds. (Plenum, New York, 1992), pp. 21–106.
30. Y. Nakamura, C. D. Chen, J. S. Tsai, *Phys. Rev. Lett.* **79**, 2328 (1997).
31. G. Johansson, e-Print available at http://xxx.lanl.gov/abs/cond-mat/0210539.
32. A. A. Clerk, S. M. Girvin, A. K. Nguyen, A. D. Stone, *Phys. Rev. Lett.* **89**, 176804 (2002).
33. We thank Y. Nakamura, K. Harmans, P. Hadley, Y. Nazarov, H. Mooij, D. Bagrets, and Y. Blanter for discussions. We acknowledge the technical assistance of R. Schouten, B. van der Enden, and M. van Oossanen. Supported by the Dutch Organisation for Fundamental Research (FOM), and U.S. Army Research Office (grant DAAD19-02-1-0700).

**Supporting Online Material**
www.sciencemag.org/cgi/content/full/301/5630/203/DC1
Materials and Methods
SOM Text
Figs. S1 and S2

5 March 2003; accepted 16 June 2003